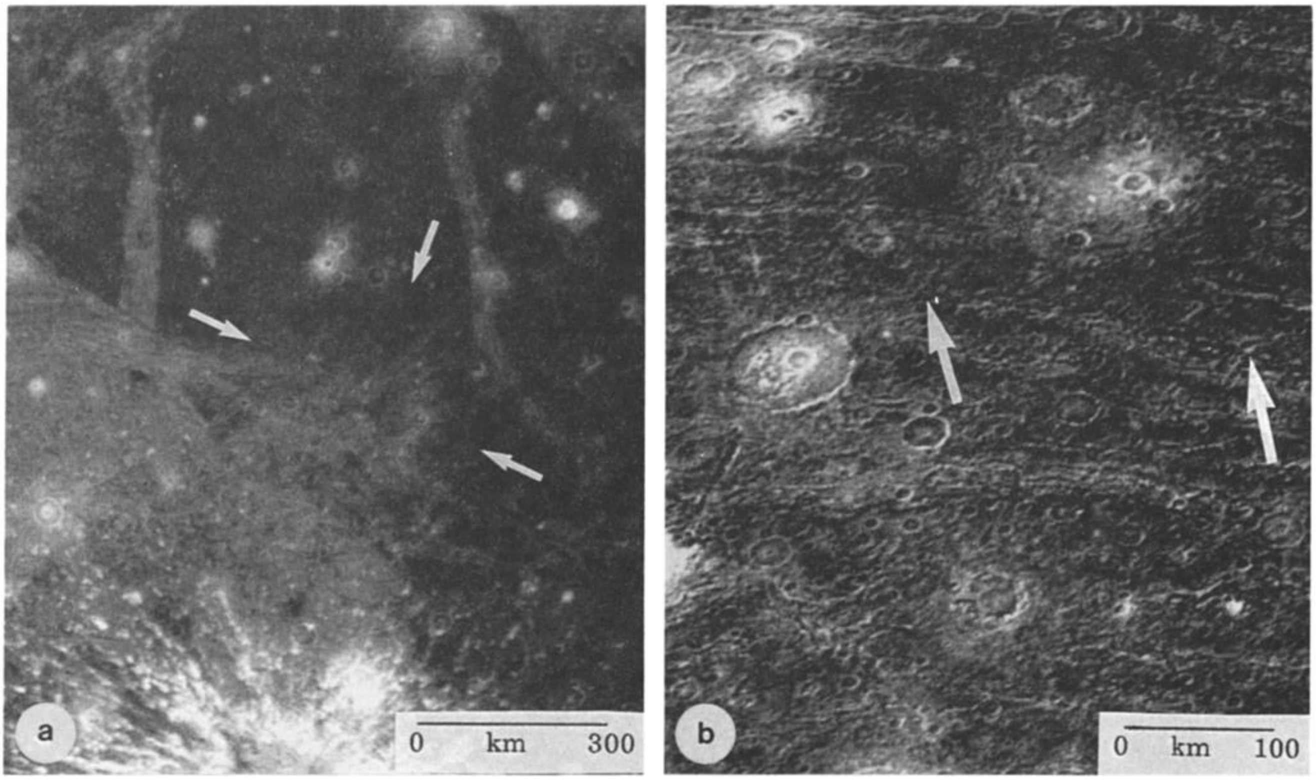

Fig. 5. (*a*) The faint giant palimpsest (shown by arrows) at the center of the furrows in the anti-Jovian hemisphere. North is up. (Voyager image 20631.23, centered near 22°S,160°W.) (*b*) Closely associated arcuate and radial furrows in Galileo Regio. The arcuate furrows trend east-southeast here, and the radial furrows trend northeast. Most radial furrows terminate against or are crosscut by the arcuate furrows, but radial furrows crosscut arcuate ones at the locations shown by arrows. North is up. (Voyager image 20636.56, centered near 33°N,159°W.)

tions, three different algorithms for weighting the contributions of furrows in different parts of area 3 were attempted. This was accomplished by separating area 3 into two subregions, east and west of about 170°W, and determining three types of furrow poles: (1) one for only the western furrow population, found to be 15°S,178°W, (2) one in which the eastern and western populations were weighted by the numbers of furrows within each, found to be 15°S,176°W, and (3) one in which the eastern and western populations were weighted by the equal azimuthal range of furrow orientations represented in each population, found to be 15°S,168°W (the pole position represented in Figure 7*c*). The latter furrow pole provides the best visual fit for furrows less than 50°-60° of arc from the center of furrow curvature, a distance beyond which *Schenk and McKinnon's* [1987] results suggest that furrow concentricity may break down.

The difference between this furrow pole and that calculated for central Marius Regio by *Schenk and McKinnon* [1987] must be be due in part to the difference in algorithms used. However, a larger part of the difference may be due to differences in the detail in which the furrows were mapped: Schenk and McKinnon's maps depict only three furrows east of approximately 190°W, as opposed to the several tens of furrows in this region shown in Figure 7*c*.

Area 4, southern Marius Regio (region "F" in Figure 7*a*), has an average furrow pole of 15°S,200°W. The difference between this pole and that calculated for the same area by *Schenk and McKinnon* [1987] may be due to use of only linear furrow segments, mapping and measurement of additional furrows, or the difference in algorithms.

System III

A detailed map of all system III furrows is shown in Figure 6. The arcuate furrows have a reasonably good visual fit to small circles centered on a pole of 60°N,50°W, in an area of light terrain north of Perrine Regio. The principal areas of furrow nonconcentricity are in northeastern Nicholson Regio and to its north, and in several small dark blocks isolated within large areas of light terrain (arrows, Figure 6). All of these areas possess one of two sets of attributes: (1) a polygonal spatial pattern of furrows similar to that observed among many younger grooves, consistent with these troughs being grooves that have cut dark terrain; or (2) a greater distance from the center of furrow curvature than 70° of arc, at which distance concentricity may break down.

Schenk and McKinnon [1987] have suggested that the arcuate furrows in system III belong to two sets. One set, in Perrine Regio, was suggested to be centered to the north at at 56°N,46°W. Another set, in Barnard Regio and Nicholson Regio, was suggested to be centered at 38°N,32°W, or alternatively between Barnard Regio and Nicholson Regio at 21°N,359°W. The hypothesis of two furrow sets, an older one centered at 38°N,32°W and a younger one in Perrine Regio, cannot be ruled out on the basis of the data in Figure 6. However, most of the furrows in Figure 6 are reasonably concentric